Deep Video Deblurring

Supplementary Material

Outline

- Full-size images in fig. 4
- Full-size images in fig. 6
- Additional comparisons with Cho [3], Kim and Lee [15], and WFA [5]
- Additional results
- Analysis on the DeBlurNet

- “**Cho [3]**”: S. Cho, J. Wang, and S. Lee. Video deblurring for hand-held cameras using patch-based synthesis. *ACM Transactions on Graphics (TOG)*, 31(4):64, 2012.
- “**Kim and Lee [15]**”: T. H. Kim and K. M. Lee. Generalized video deblurring for dynamic scenes. In *Proc. IEEE Conf. Comput. Vis. Pattern Recognit. (CVPR)*, 2015.
- “**WFA [5]**”: M. Delbracio and G. Sapiro. Hand-held video deblurring via efficient fourier aggregation. *IEEE Transactions on Computational Imaging*, 1(4):270–283, 2015.
- “**L0Deblur [48]**”: L. Xu, S. Zheng, and J. Jia. Unnatural l0 sparse representation for natural image deblurring. In *Proceedings of the IEEE Conference on Computer Vision and Pattern Recognition*, pages 1107–1114, 2013.
- “**Neural [1]**”: A. Chakrabarti. A neural approach to blind motion deblurring. *arXiv preprint arXiv:1603.04771*, 2016.

Full-size Images in Fig. 4

input

PSDeblur

WFA [5]

DBN+Single

DBN+Noalign

DBN+Homog

DBN+Flow

ground-truth

input

PSDeblur

WFA [5]

DBN+Single

DBN+Noalign

DBN+Homog

DBN+Flow

ground-truth

Full-size Images in Fig. 6

input

L0Deblur [48]

Neural [1]

WFA [5]

DBN+Single

DBN+Noalign

DBN+Homog

DBN+Flow

input

L0Deblur[48]

Neural [1]

WFA [5]

DBN+Single

DBN+Noalign

DBN+Homog

DBN+Flow

input

PSDeblur

Cho [3]

Kim and Lee [15]

WFA [5]

DBN+Single

DBN+Noalign

DBN+Homog

DBN+Flow

input

PSDeblur

Cho [3]

Kim and Lee [15]

WFA [5]

DBN+Single

DBN+Noalign

DBN+Homog

DBN+Flow

Additional Comparisons with Cho [3], Kim and Lee [15], and WFA [5]

input

Cho [3]

Kim and Lee [15]

WFA [5]

DBN+Single

DBN+Noalign

DBN+Homog

DBN+Flow

input

Cho [3]

Kim and Lee [15]

WFA [5]

DBN+Single

DBN+Noalign

DBN+Homog

DBN+Flow

input

Cho [3]

Kim and Lee [15]

WFA [5]

DBN+Single

DBN+Noalign

DBN+Homog

DBN+Flow

Additional Results

input

DBN+Noalign

DBN+Homog

DBN+Flow

input

DBN+Noalign

DBN+Homog

DBN+Flow

input

DBN+Noalign

DBN+Homog

DBN+Flow

input

DBN+Noalign

DBN+Homog

DBN+Flow

input

DBN+Noalign

DBN+Homog

DBN+Flow

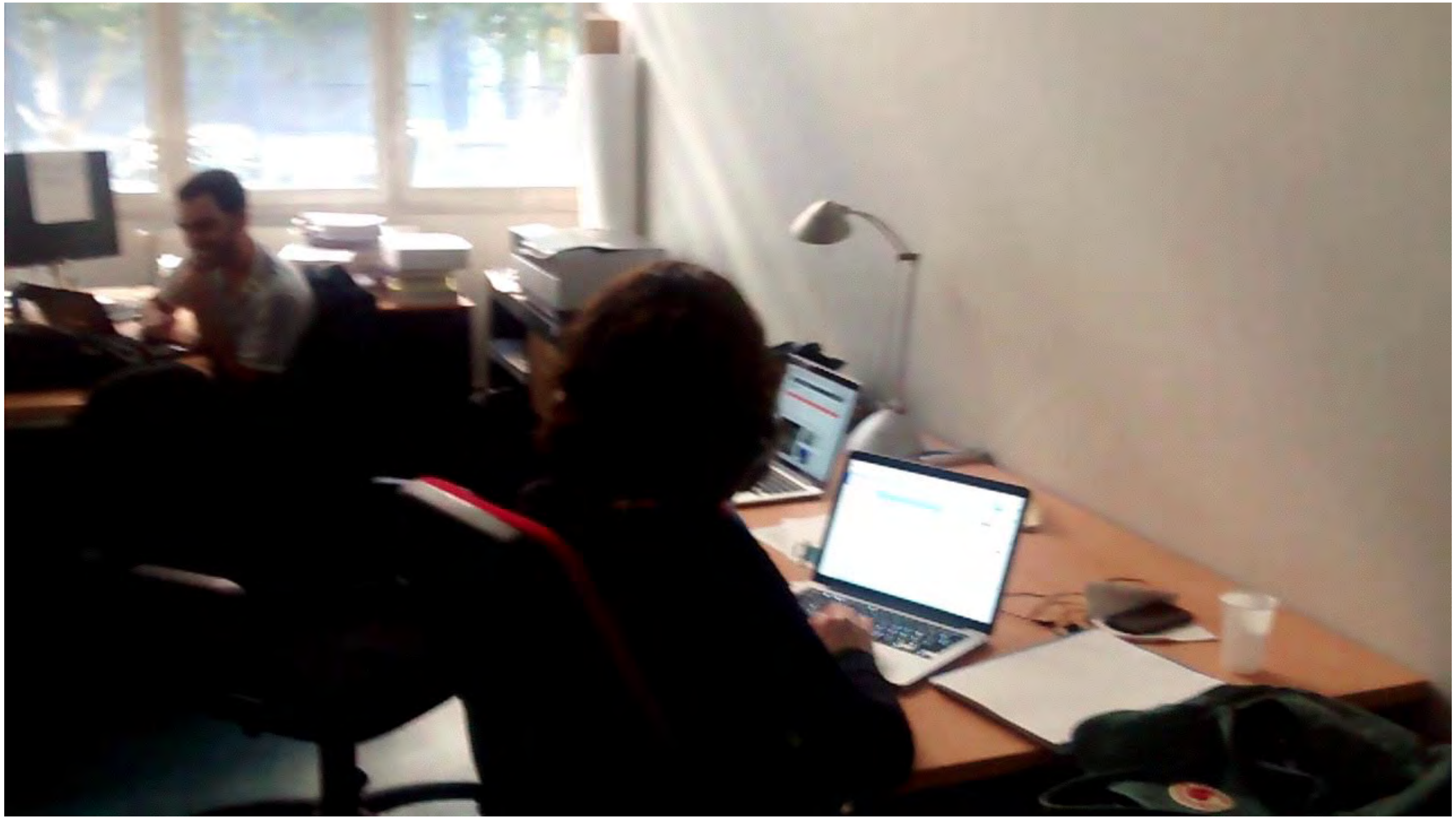

input

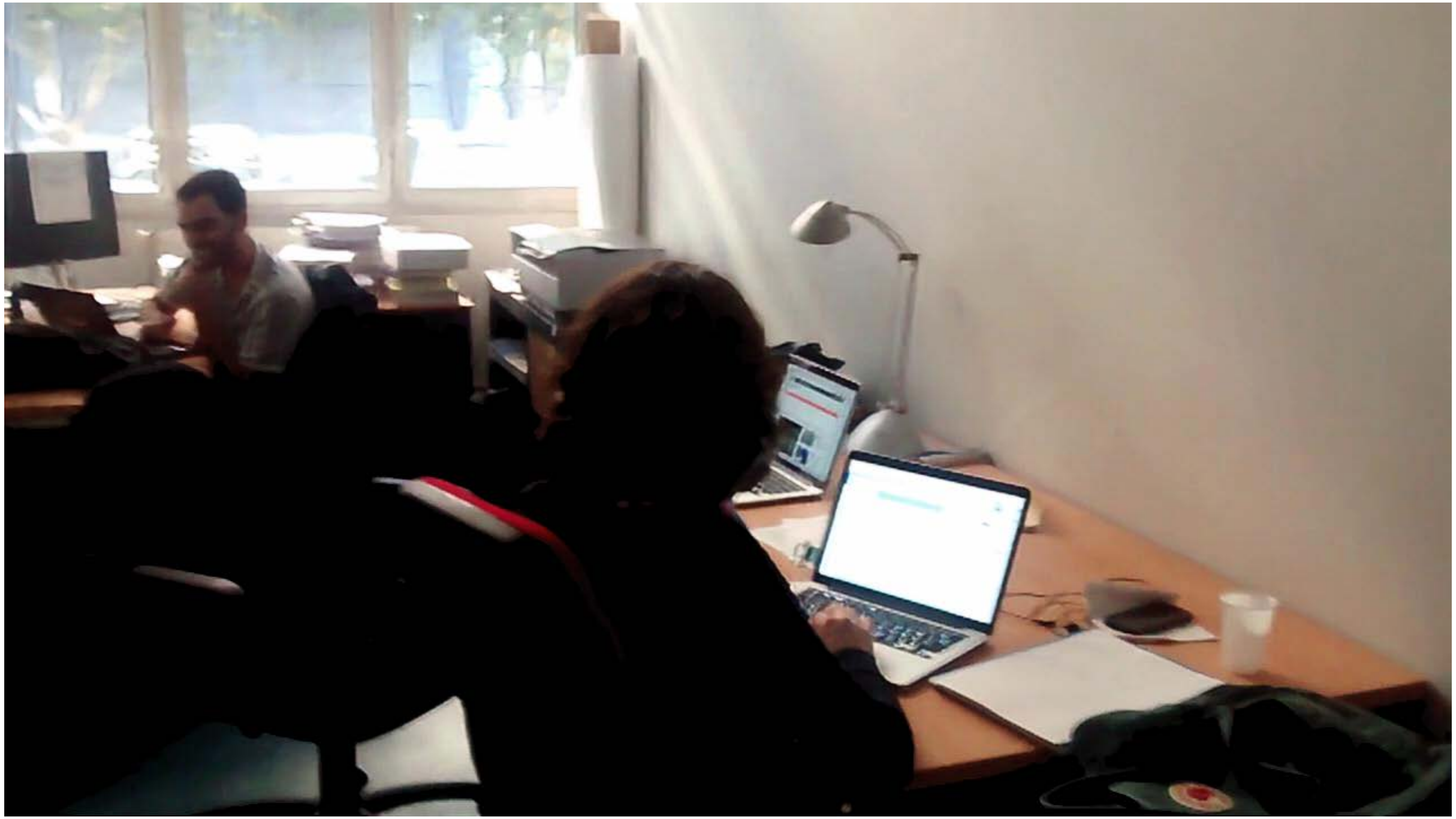

DBN+Noalign

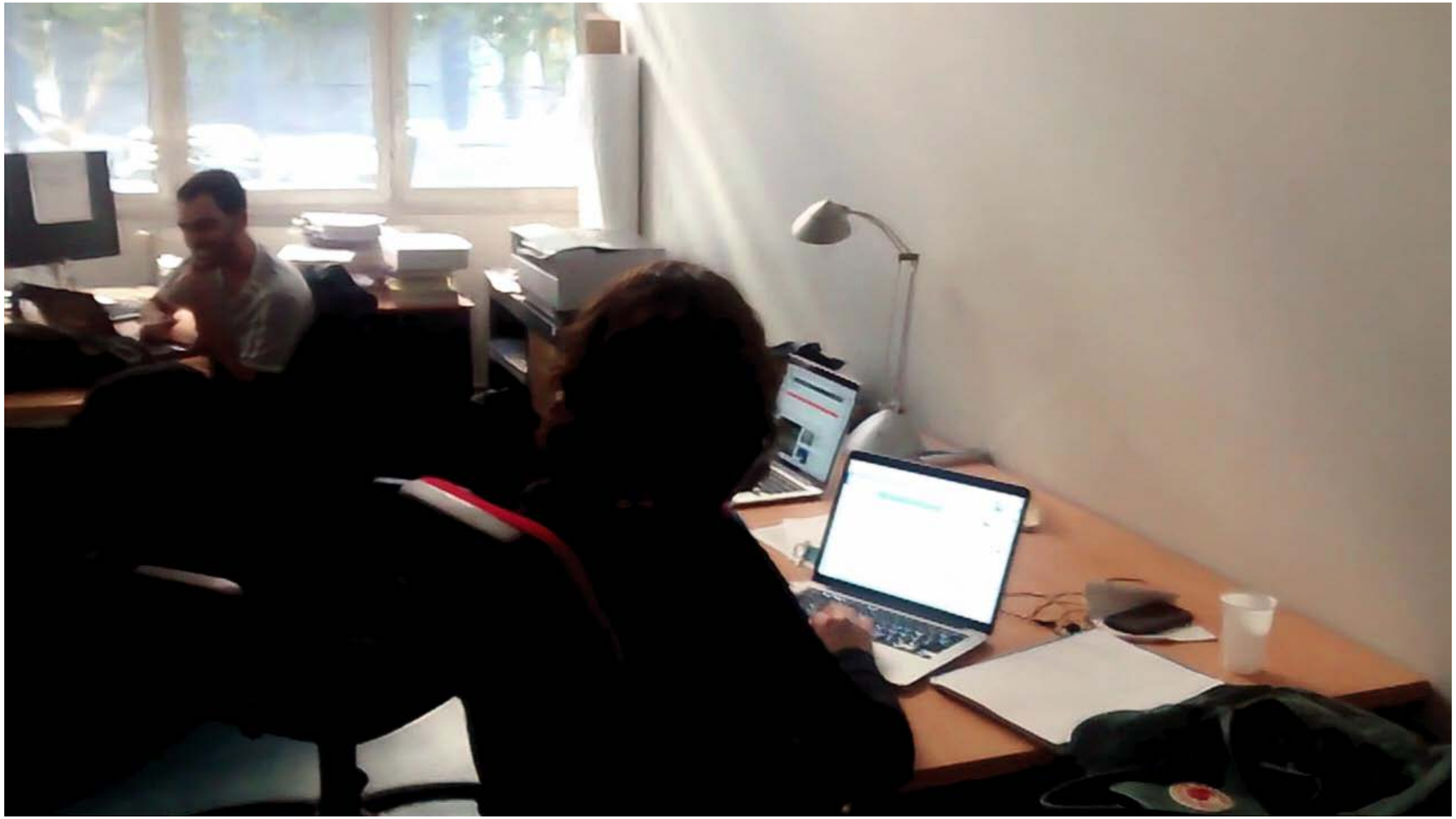

DBN+Homog

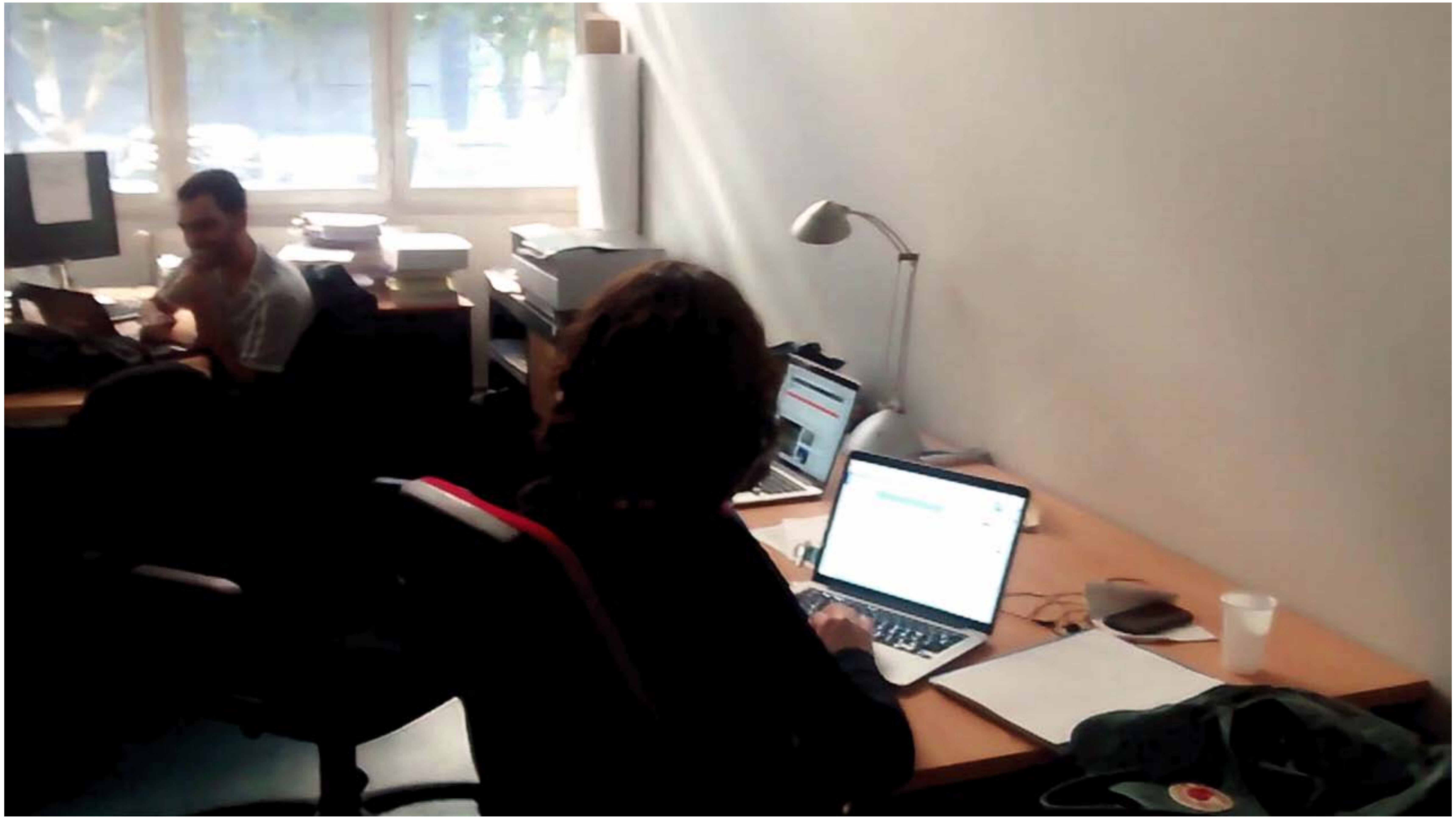

DBN+Flow

input

DBN+Noalign

DBN+Homog

DBN+Flow

input

DBN+Noalign

DBN+Homog

DBN+Flow

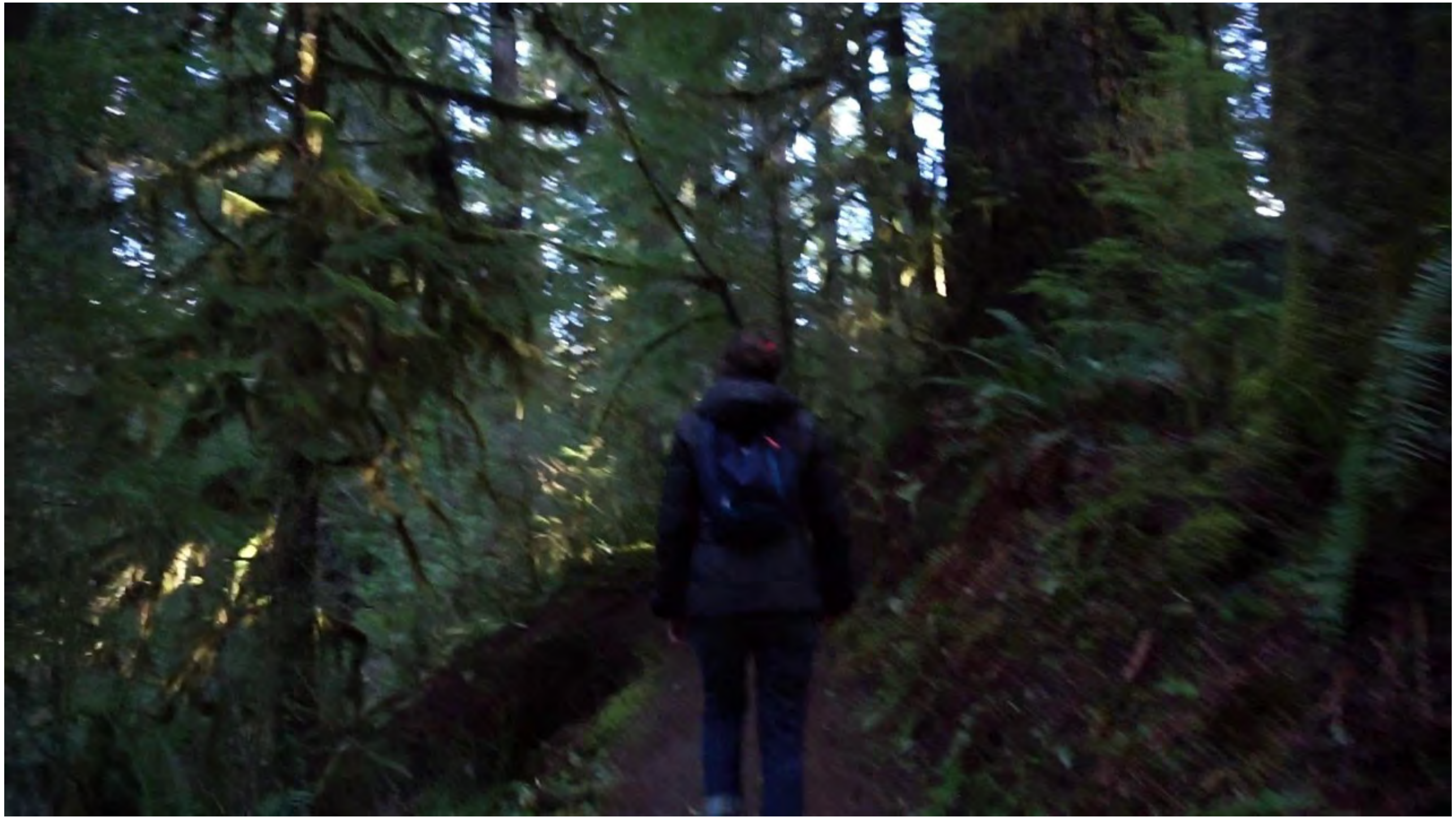

input

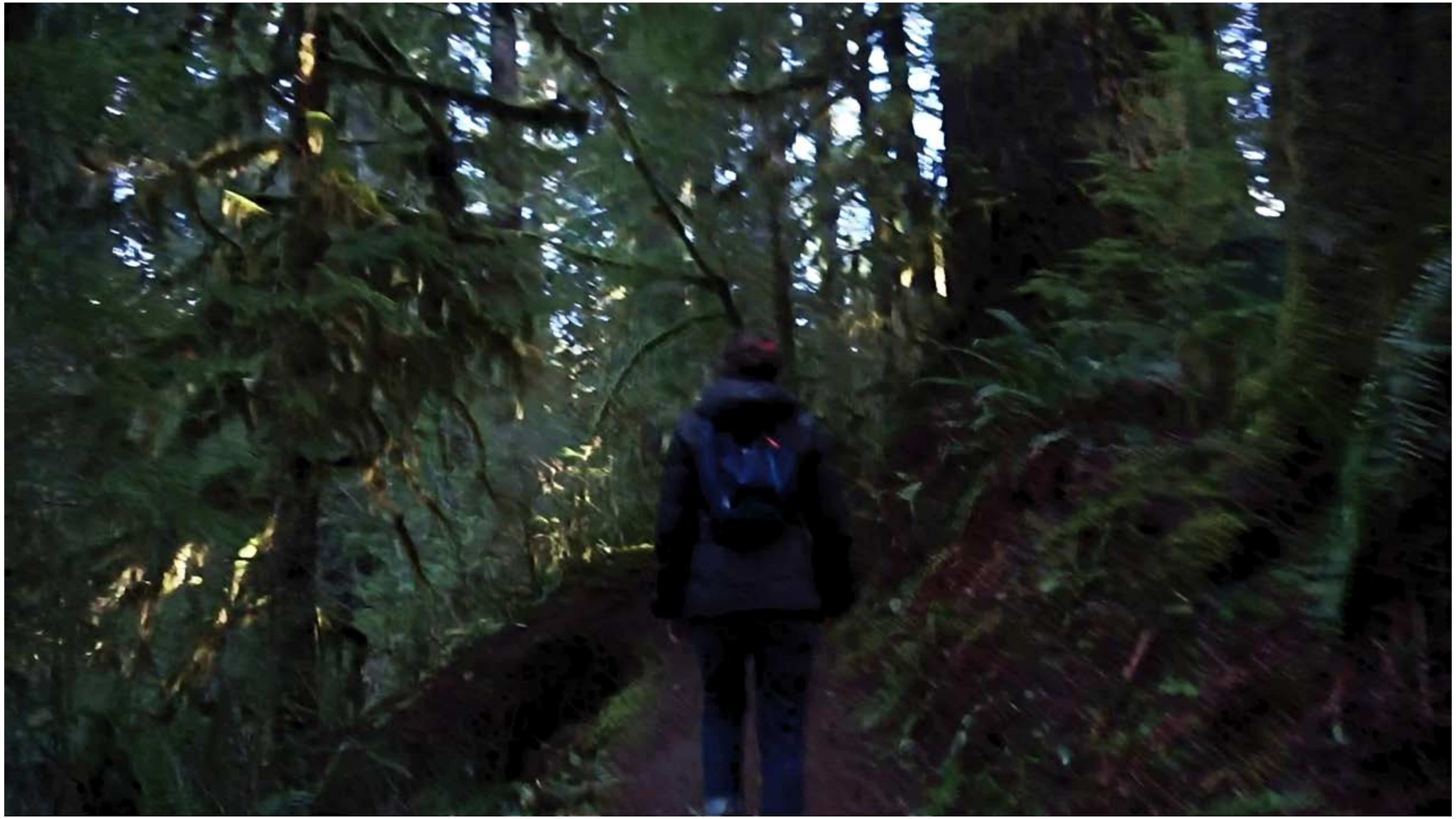

DBN+Noalign

DBN+Homog

DBN+Flow

input

DBN+Noalign

DBN+Homog

DBN+Flow

Analysis on DeBlurNet

Depth of DBN

- Here we compare DBN with a slightly shallower version, where D3 to F4_3 are removed. The bottleneck layers in DBN greatly help with handling misalignment and aggregation.

DBN-Shallower+Flow

DBN+Flow

Late v.s. Early Fusion

- Here we compare different fusion strategies. While late fusion occasionally helps with challenging cases where DBN+Noalign fails, this improvement is not consistent. This might be related to the failure of artifacts/misalignments detections without the presence of reference frame.

DBN-LateFusion+Noalign

DBN+Noalign

Visualization of Filters Learned

- Here we visualize some filters learned from DBN, specifically at F0. It can be observed that DBN not only learns to locate the corresponding color channels in the input stack, but is also able to learn to extract edges of different orientations, and to locate the warping artifacts.

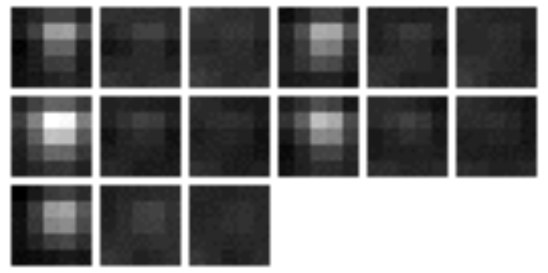

Filters and responses from F0 at DBN+Flow, that appear to find color channel correspondences.

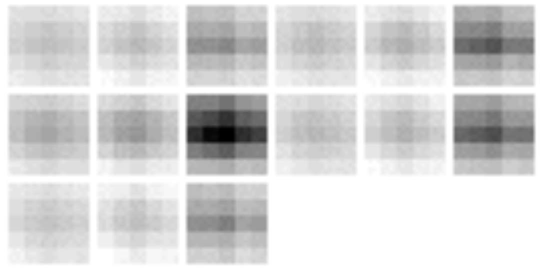

Filters and responses from F0 at DBN+Flow, that appear to find color channel correspondences.

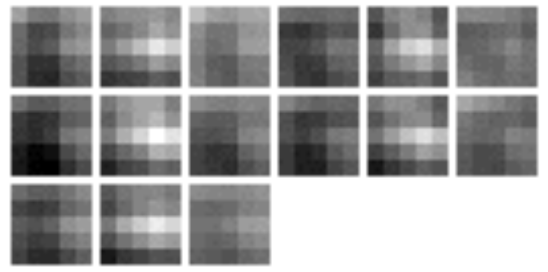

Filters and responses from F0 at DBN+Flow, that appear to find edges.

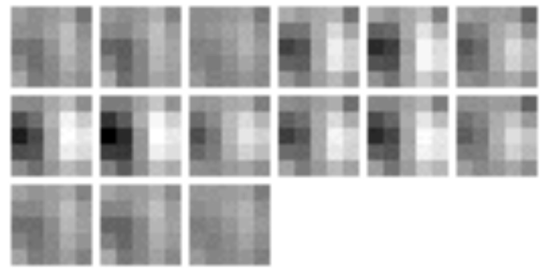

Edges

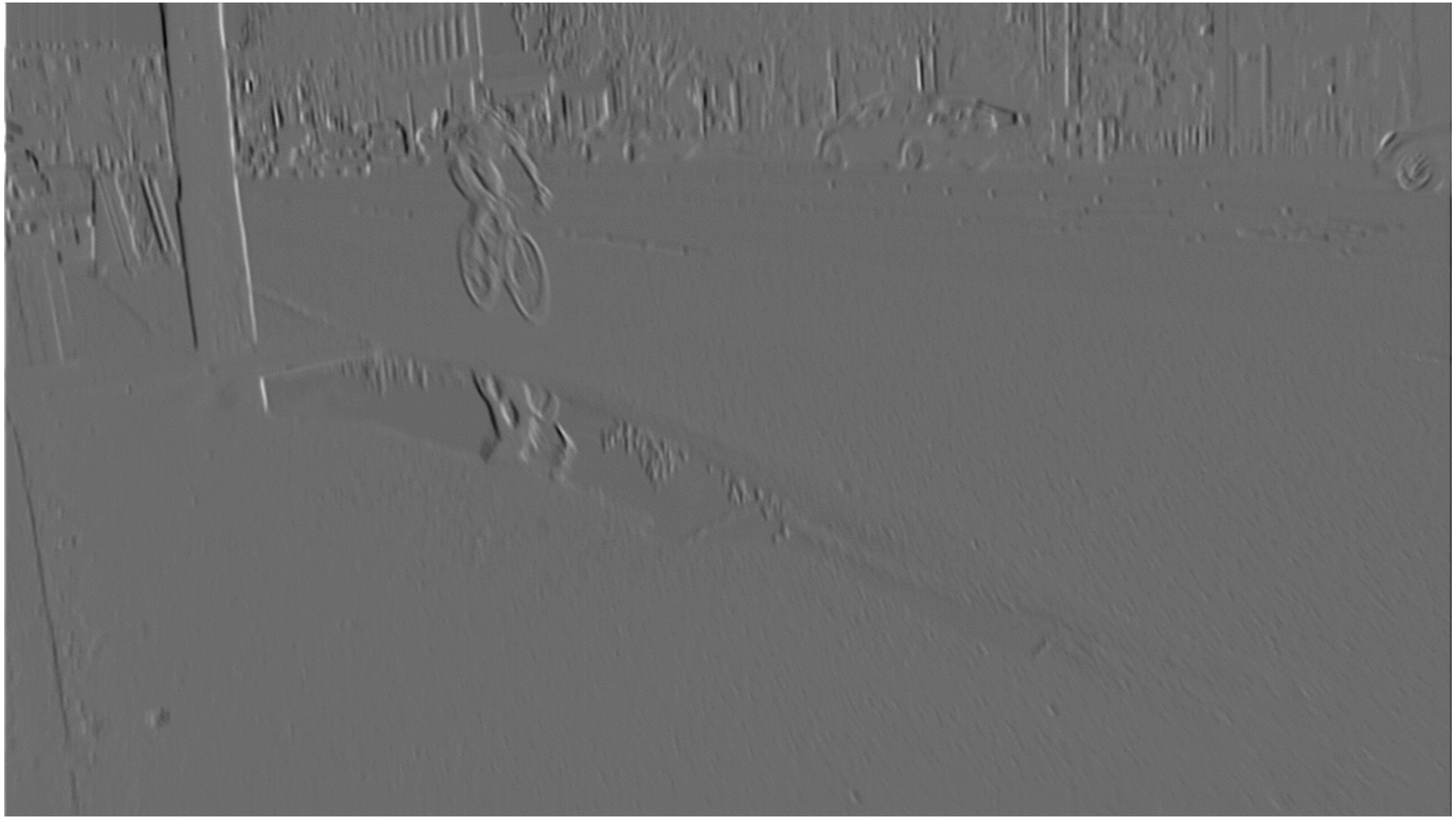

Filters and responses from F0 at DBN+Flow, that appear to find edges.

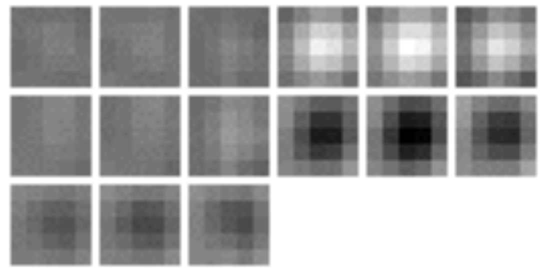

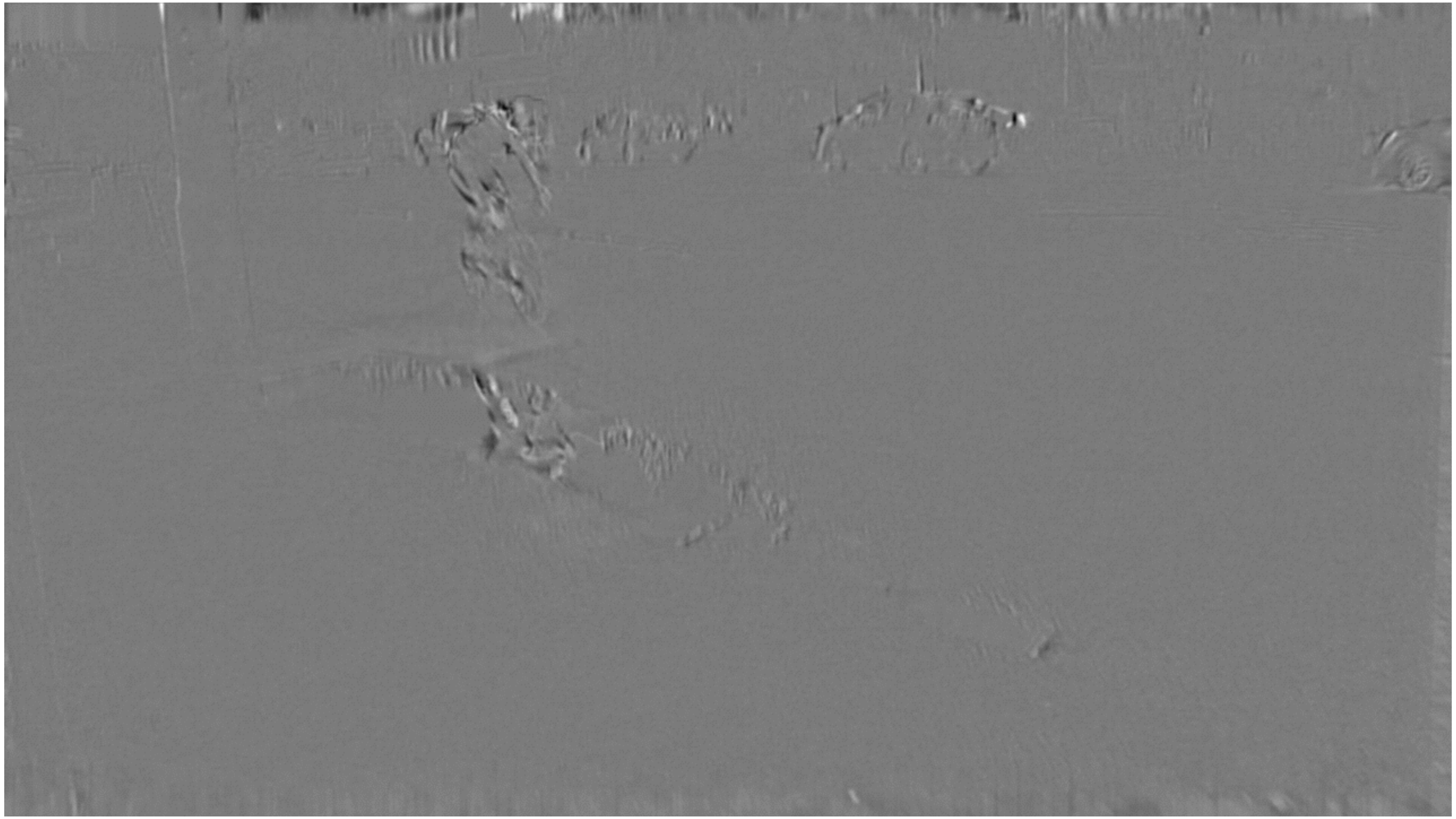

Filters and responses from F0 at DBN+Flow, that appear to detect warping artifacts.

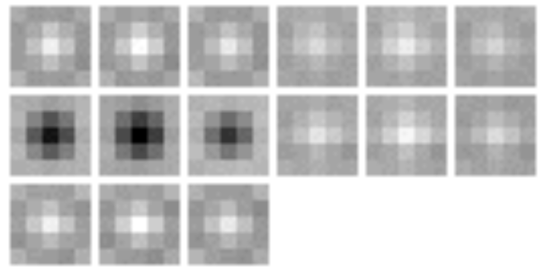

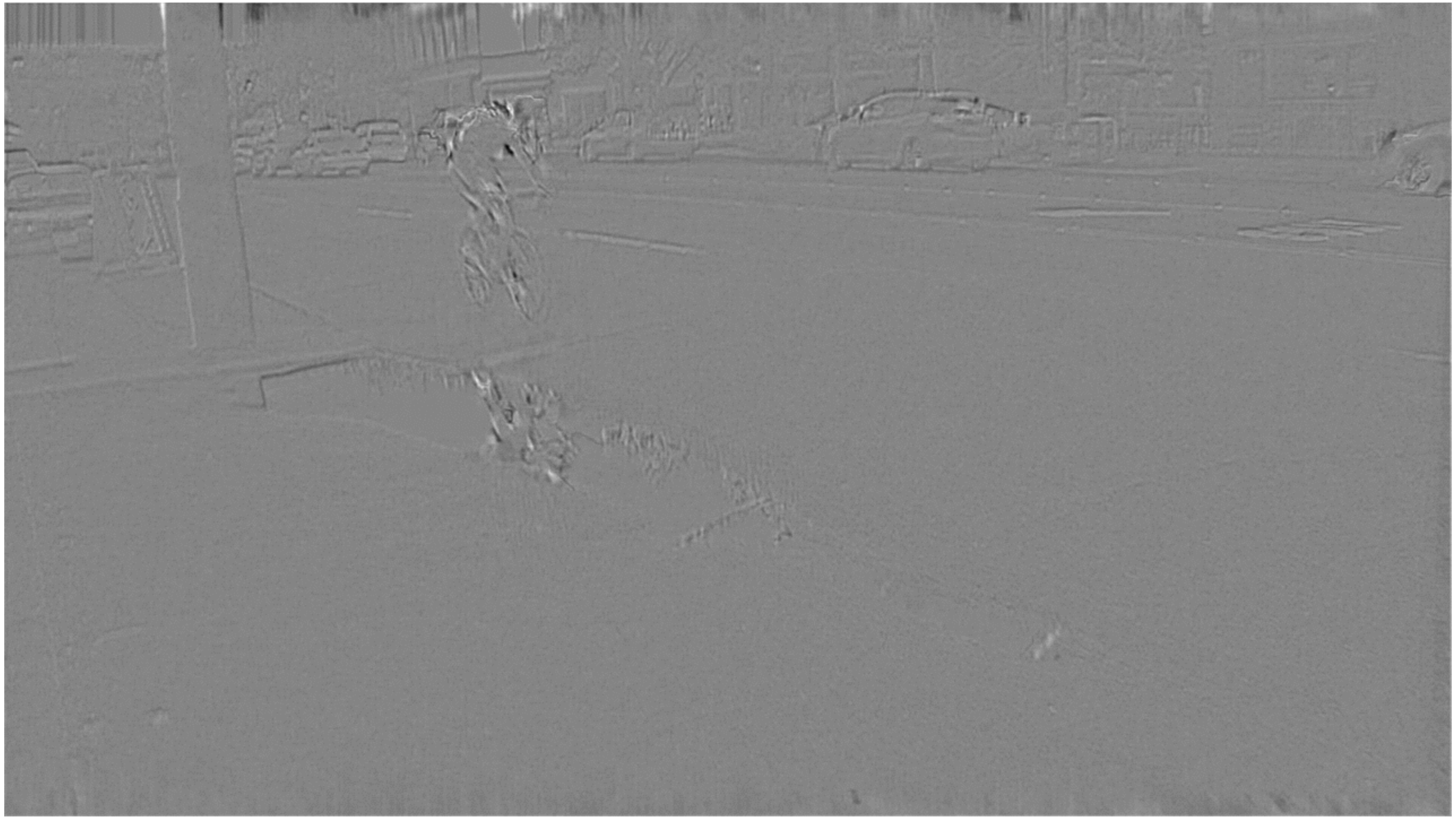

Filters and responses from F0 at DBN+Flow, that appear to detect warping artifacts.

Convergence

- A convergence plot is given here.

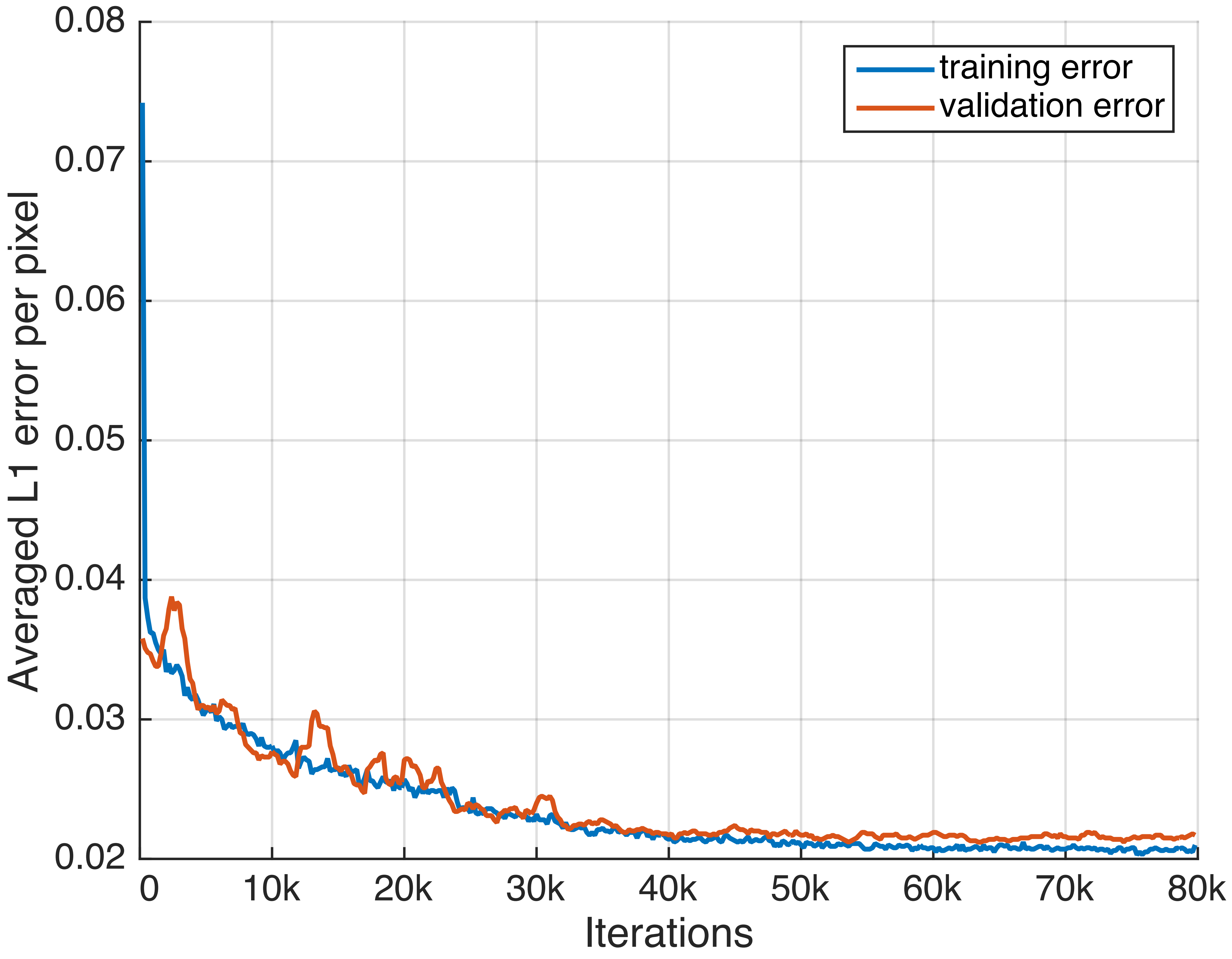

Convergence, DBN+Flow